Supporting Information

Electrically Reading a Light-Driven Molecular Switch on 2D-$Ti_3C_2T_x$ MXene: Towards Responsive MXetronics

Jose Muñoz, Mario Palacios-Corella, Martin Pumera*

Supporting Figures

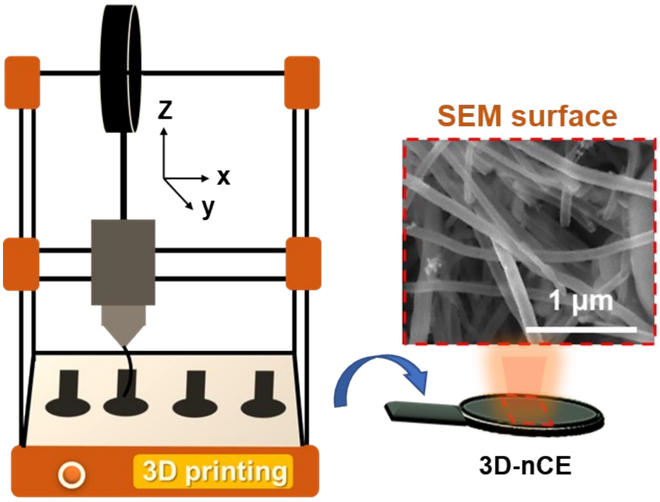

Figure S1. 3D-printing setup employed for 3D-nCE fabrication. 3D-nCE were manufactured by fused deposition modeling technology using a Prusa i3 MK3 printer (Prusa Research, Czech Republic). Briefly, a commercially available graphene/polylactic acid nanocomposite filament (Black Magic 3D filament, USA) was utilized as the conductive material. For the printing, the filament was extruded down through the nozzle (0.4 mm) at 215 ºC (bed temperature: 60 ºC). The geometric area of the 3D-nCE (corresponding to the spheric part of the device, as depicted in the illustration) was 0.28 cm^2. To electrically activate the 3D-nCE, the electrode was immersed in DMF for 180 min in order to partially remove the insulating polylactic acid polymer of the electrode surface. Inset: Morphological image of the activated 3D-nCE surface taken by SEM.

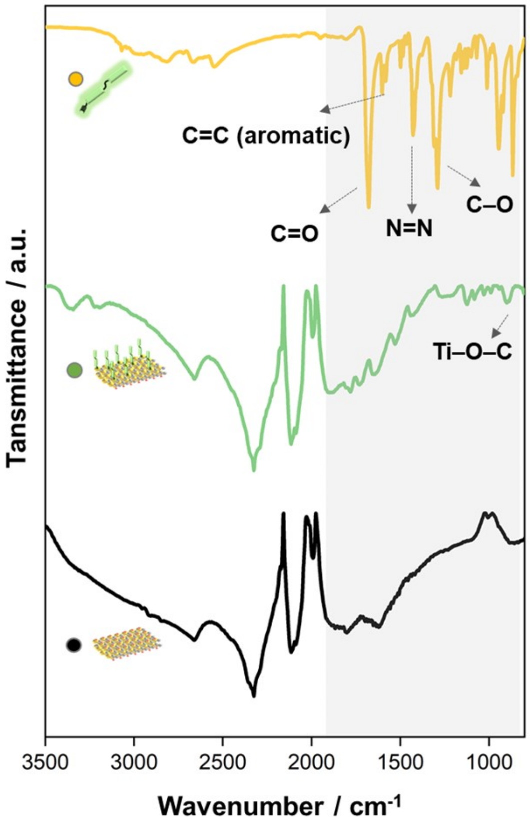

Figure S2. FTIR spectra of pristine $Ti_3C_2T_x$, functionalized AZO@$Ti_3C_2T_x$ and raw AZO molecule. The basic characteristic peaks of raw AZO molecule were identified in the region from 1700 to 850 cm^{-1}, which includes the stretching vibration of C=O at 1685 cm^{-1}, the stretching vibration of C=C at 1569 cm^{-1}, the stretching vibration of N=N at 1420 cm^{-1} and the stretching vibration of C–O at 1278 cm^{-1}. Such characteristic features observed in that region were clearly transferred to photo-responsive AZO@$Ti_3C_2T_x$. Further, the new peak at 886 cm^{-1} in the AZO@$Ti_3C_2T_x$, which corresponds to the stretching vibration of Ti-O-C, elucidates the covalent nature of the grafting.

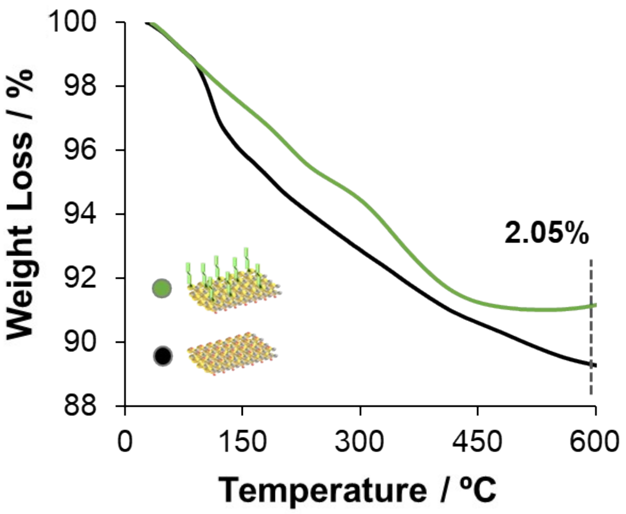

Figure S3. TGA curves of pristine 2D-$Ti_3C_2T_x$ and functionalized AZO@$Ti_3C_2T_x$. Analyses were carried out in a N_2 atmosphere with a ramp temperature of 10 ºC·min^{-1}.

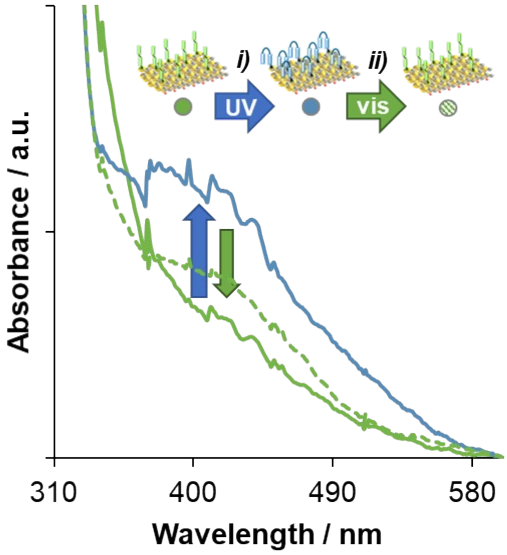

Figure S4. Optical properties of the photo-responsive AZO@$Ti_3C_2T_x$. UV-vis spectra of the photo-responsive AZO@$Ti_3C_2T_x$ before and after irradiating the material with *i)* UV light and *ii)* green light for 15 min to promote a reversible bistable molecular switch (*E*–AZO@$Ti_3C_2T_x$ ↔ *Z*–AZO@$Ti_3C_2T_x$).

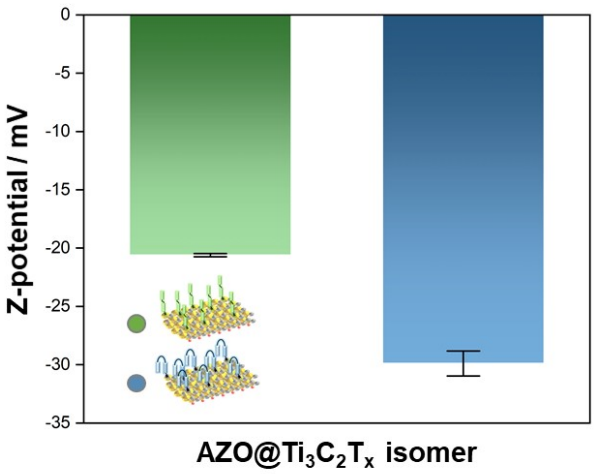

Figure S5. Z-potential of the photo-responsive AZO@Ti$_3$C$_2$T$_x$ at the two different states. ζ-potential (in mV) of the photo-responsive AZO@Ti$_3$C$_2$T$_x$ before (*E*–AZO@Ti$_3$C$_2$T$_x$) and after irradiating with UV light for 15 min (*Z*–AZO@Ti$_3$C$_2$T$_x$). This change is in line with the straight-to-bent transition of AZO molecule. Accordingly, a lower ζ-potential value is expected after UV light irradiation since the charge is confined in a lower particle size, resulting in a decrease from –20.6 ± 0.1 mV (*E*–AZO@Ti$_3$C$_2$T$_x$) to –29.9 ± 0.7 mV (*Z*–AZO@Ti$_3$C$_2$T$_x$). Experiments were run per triplicate (*n = 3*) using a Malvern Zetasaizer (solvent: deionized water; material concentration: 0.01 mg·mL^{-1}).

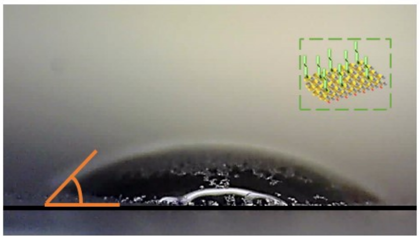
θ = 49.6 ± 0.2º

Figure S6. Reversibility of the water contact angle after green light irradiation. After irradiating the previous *Z*–AZO@$Ti_3C_2T_x$ form with visible light for 15 min (in order to promote the *Z/E* transition), the resulting *E*–AZO@$Ti_3C_2T_x$ exhibited a water contact angle value of 49.6 ± 0.2º. This value is higher than the one achieved by the photo-responsive AZO@$Ti_3C_2T_x$ after UV irradiation (44 ± 1º) and close to the one exhibited before UV irradiation (51.2 ± 0.7º).

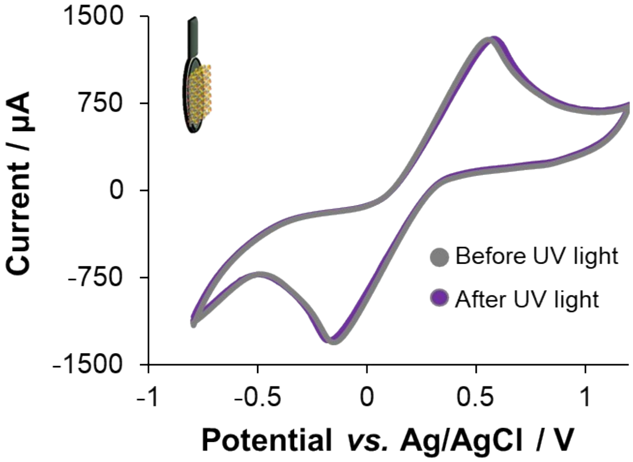

Figure S7. Control electrochemical experiment at the MXetronic made of pristine 2D-$Ti_3C_2T_x$. CV at the control MXetronic before and after UV light irradiation for 15 min, demonstrating that no significant electrochemical changes by means of *ΔE* and *Ip* values can be reached without the presence of the photo-responsive AZO molecule.